Contents

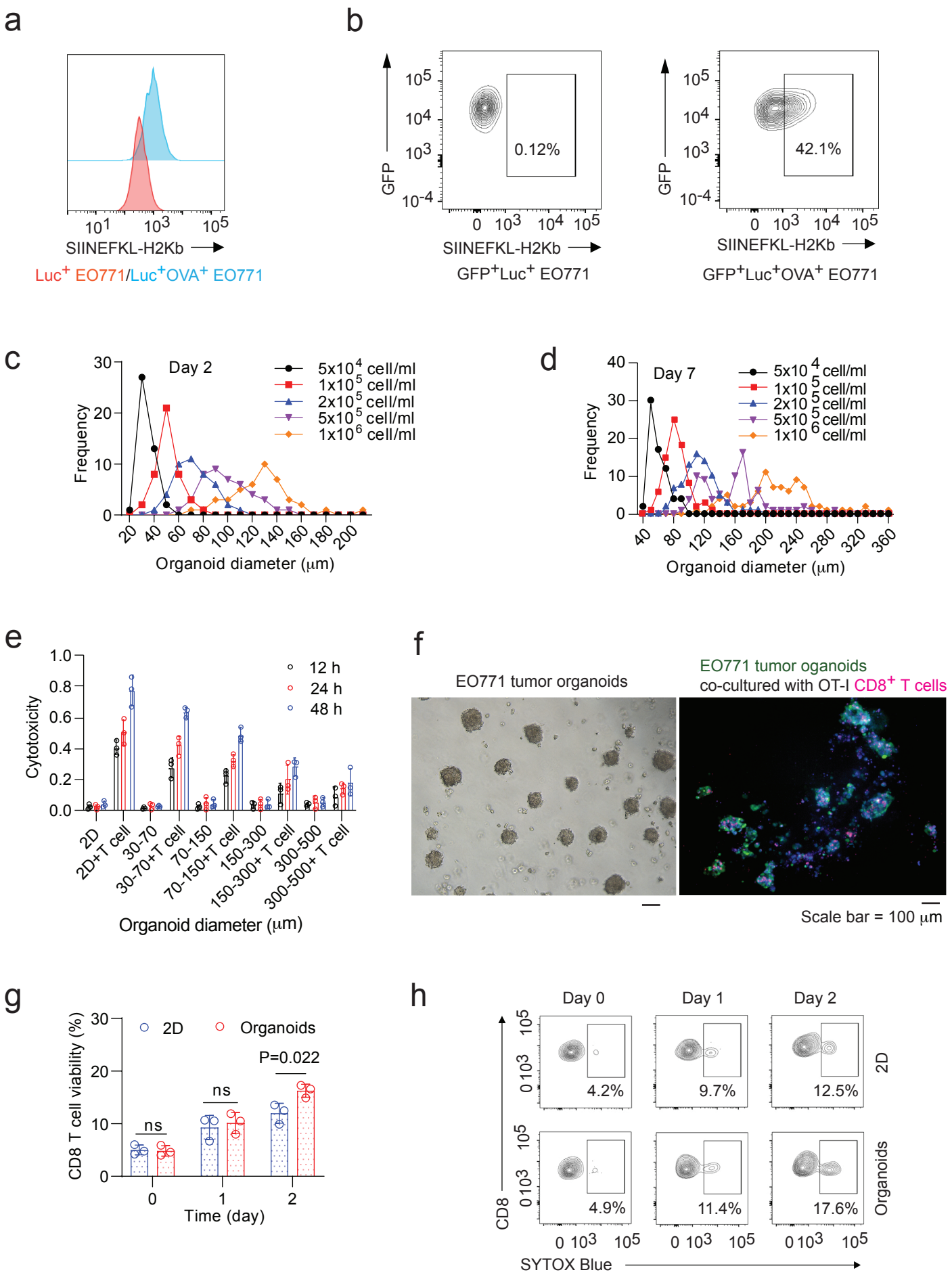
a
SIINEFKL-H2Kb
Luc+ EO771/Luc+OVA+ EO771
b
GFP
0.12%
SIINEFKL-H2Kb
GFP+Luc+ EO771
42.1%
GFP+Luc+OVA+ EO771
c
Day 2
Frequency
5x10^4 cell/ml
1x10^5 cell/ml
2x10^5 cell/ml
5x10^5 cell/ml
1x10^6 cell/ml
Organoid diameter (μm)
d
Day 7
Frequency
5x10^4 cell/ml
1x10^5 cell/ml
2x10^5 cell/ml
5x10^5 cell/ml
1x10^6 cell/ml
Organoid diameter (μm)
e
Cytotoxicity
12 h
24 h
48 h
2D
2D+T cell
30-70
30-70+T cell
70-150
70-150+T cell
150-300
150-300+ T cell
300-500
300-500+ T cell
Organoid diameter (μm)
f
EO771 tumor organoids
EO771 tumor oganoids
co-cultured with OT-I CD8+ T cells
Scale bar = 100 μm
g
CD8 T cell viability (%)
2D
Organoids
P=0.022
ns
ns
Time (day)
h
Day 0
Day 1
Day 2
4.2%
9.7%
12.5%
4.9%
11.4%
17.6%
2D
Organoids
CD8
SYTOX Blue

Supplementary Fig. 1 | Characterization and optimization of EO771 tumour organoids. **a,** Levels of OVA antigen on EO771 and OVA^+ EO771 cells, determined by mean fluorescence intensity (MFI) in flow cytometry. **b**, Flow cytometry analysis showing OVA antigen levels on Luc^+OVA^+ EO771 cells and $GFP^+Luc^+OVA^+$ EO771 cells. A total of 10,000 events per sample were collected. Doublets and dead cells were excluded from data analysis. **c,d,** Size distributions of EO771 tumour organoids with varying seeding cell concentrations and culture times. **e**, $CD8^+$ T cell-mediated cytotoxicity on mouse $GFP^+Luc^+OVA^+$ EO771 cells in 2D cell culture (with or without T cells) and 3D tumour organoids (with T cells) with different sizes for indicated culture time. Error bar indicates SD of three independent samples. **f**, Optical images showed EO771 tumour organoids with size of 70-150 μm in diameter in culture. Immunofluorescence images showed that EO771 tumour organoids were co-cultured with and without $CD8^+$ T cells from OT-I mice. EO771 tumour cells are visible in green colour (GFP^+). $CD8^+$ T cells were stained with APC-conjugated anti-mouse CD8 and shown in red colour. **g**, The death proportions of OVA-specific $CD8^+$ T cells co-cultured with $GFP^+Luc^+OVA^+$ EO771 cells (2D) and $GFP^+Luc^+OVA^+$ EO771 tumour organoids. Two-way ANOVA test was used for data analysis (**g**). Data from three biologically parallel experiments are presented as mean ± SD. ns, no significance. **h**, Representative flow cytometry data showing death proportions of OVA-specific $CD8^+$ T cells co-cultured with $GFP^+Luc^+OVA^+$ EO771 cells (2D) and $GFP^+Luc^+OVA^+$ EO771 tumour organoids. Death proportions of $CD8^+$ T cells were measured at day 0, 1 and 2. SYTOX Blue reagent was used to stain dead cells.

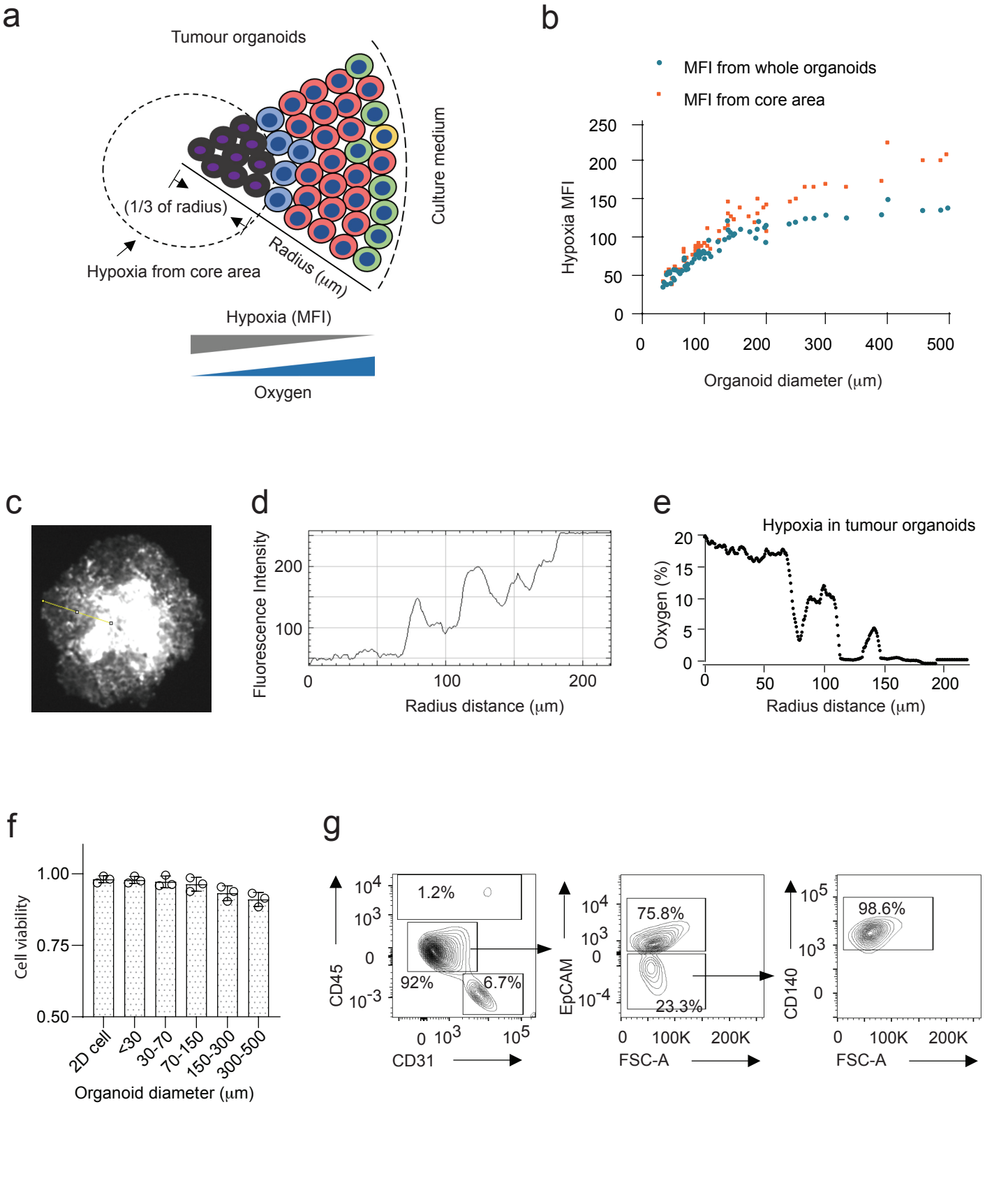
a
Tumour organoids
Culture medium
(1/3 of radius)
Radius (μm)
Hypoxia from core area
Hypoxia (MFI)
Oxygen
b
MFI from whole organoids
MFI from core area
Hypoxia MFI
Organoid diameter (μm)
c
d
Fluorescence Intensity
Radius distance (μm)
e
Hypoxia in tumour organoids
Oxygen (%)
Radius distance (μm)
f
Cell viability
2D cell
<30
30-70
70-150
150-300
300-500
Organoid diameter (μm)
g
CD45
CD31
1.2%
92%
6.7%
EpCAM
FSC-A
75.8%
23.3%
CD140
98.6%

Supplementary Fig. 2 | Characterization of EO771 tumour organoids.

a, Schematic illustration showing how hypoxia in tumour organoids was measured in our experiments. Specifically, the hypoxia-caused fluorescence intensity of the whole and core area of tumour organoids was quantified using ImageJ software after tumour organoids were stained by the Image-iT Green Hypoxia reagent and imaged under a Leica DM4B microscope. The core area was defined as the 1/3 of the inner part of the tumour organoids, which is more representative than the whole area for hypoxia in tumour organoids. The hypoxia-caused fluorescence intensity increases from surface to center of a tumour organoid due to the decreasing oxygen delivered from culture medium. **b,** Histogram of hypoxia-caused fluorescence intensity from tumour organoids, where the mean fluorescence intensity of the whole and core area of tumour organoids was measured. The fluorescence images without optical light were analyzed by ImageJ software to determine the fluorescence intensity. **c,** Typical image showing the hypoxia-caused fluorescence intensity from surface to center of a tumour organoid. **d,** The gradient line of the fluorescence intensity shown in (**c**), reflecting the hypoxia levels from the surface to the center of a tumour organoid. **e,** The oxygen levels of the core area of tumour organoids calculated from (**d**). **f,** Tumour cell viability in the EO771 tumour organoids with different sizes. **g,** The flow cytometry gating strategy for analysis of the cellular composition of tumour organoids.

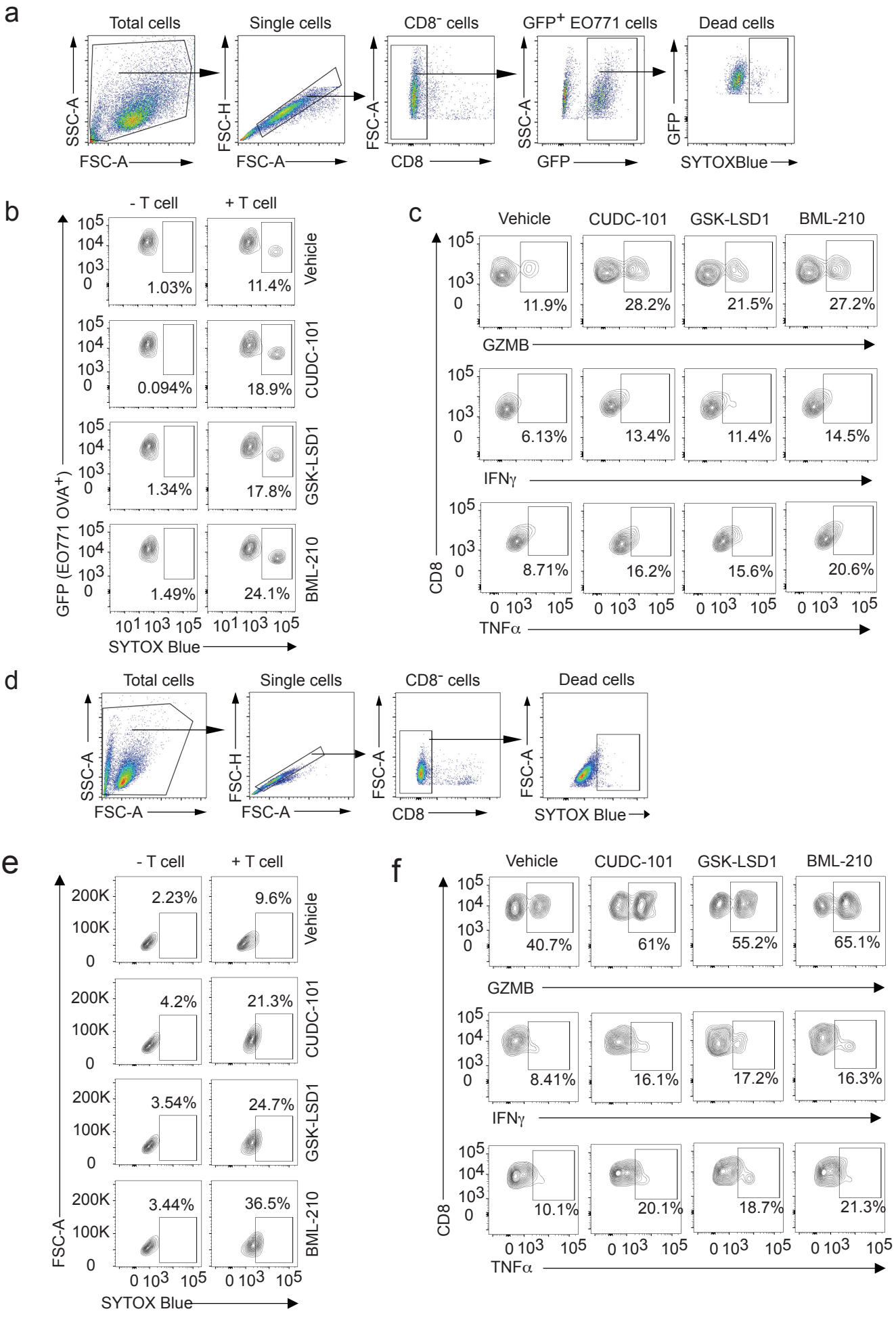
a
Total cells
Single cells
CD8⁻ cells
GFP⁺ EO771 cells
Dead cells
SSC-A
FSC-A
FSC-H
FSC-A
FSC-A
CD8
SSC-A
GFP
GFP
SYTOXBlue
b
- T cell
+ T cell
Vehicle
CUDC-101
GSK-LSD1
BML-210
1.03%
11.4%
0.094%
18.9%
1.34%
17.8%
1.49%
24.1%
GFP (EO771 OVA⁺)
SYTOX Blue
c
Vehicle
CUDC-101
GSK-LSD1
BML-210
11.9%
28.2%
21.5%
27.2%
GZMB
6.13%
13.4%
11.4%
14.5%
IFNγ
8.71%
16.2%
15.6%
20.6%
CD8
TNFα
d
Total cells
Single cells
CD8⁻ cells
Dead cells
SSC-A
FSC-A
FSC-H
FSC-A
FSC-A
CD8
FSC-A
SYTOX Blue
e
- T cell
+ T cell
Vehicle
CUDC-101
GSK-LSD1
BML-210
2.23%
9.6%
4.2%
21.3%
3.54%
24.7%
3.44%
36.5%
FSC-A
SYTOX Blue
f
Vehicle
CUDC-101
GSK-LSD1
BML-210
40.7%
61%
55.2%
65.1%
GZMB
8.41%
16.1%
17.2%
16.3%
IFNγ
10.1%
20.1%
18.7%
21.3%
CD8
TNFα

Supplementary Fig. 3 | $CD8^+$ T cell cytotoxicity in the co-cultures with mouse and human tumour organoids.

a, Flow cytometry gating strategy for the analysis of dead cells from $GFP^+Luc^+OVA^+$ EO771 tumour organoids. **b,** Representative flow cytometry data showing death proportion of $GFP^+Luc^+OVA^+$ EO771 tumour cells from the tumour organoids co-cultured with OVA-specific $CD8^+$ T cells. Tumour organoids were treated with drug in advance for 48 h and were then co-cultured with activated $CD8^+$ T cells (from OT-I mouse) for 24 h. SYTOX Blue was used to stain dead cells. **c,** Representative flow cytometry data showing active $CD8^+$ T cells in the co-culture with EO771 tumour organoids, indicated by positivity for GZMB, IFNγ and TNF-α. **d,** Flow cytometry gating strategy for analysis of dead cells from NY-ESO-1^+ MDA-MB-468 tumour organoids. **e,** Representative flow cytometry data showing death proportion of NY-ESO-1^+ MDA-MB-468 cells from tumour organoids co-cultured with NY-ESO-1-specific $CD8^+$ T cells. **f,** Representative flow cytometry data showing active $CD8^+$ T cells in the co-culture with MDA-MB-468 tumour organoids, indicated by positivity for GZMB, IFNγ and TNF-α. A total of 20,000 of events per cell sample were collected for flow cytometry analysis.

a

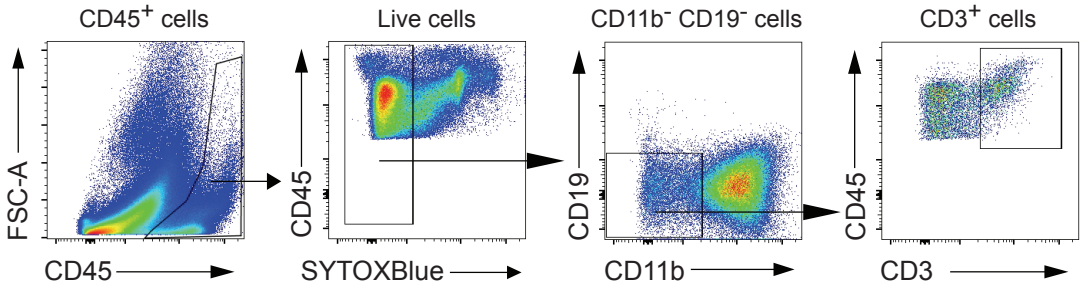
CD45+ cells
Live cells
CD11b- CD19- cells
CD3+ cells
FSC-A
CD45
CD45
SYTOXBlue
CD19
CD11b
CD45
CD3

b

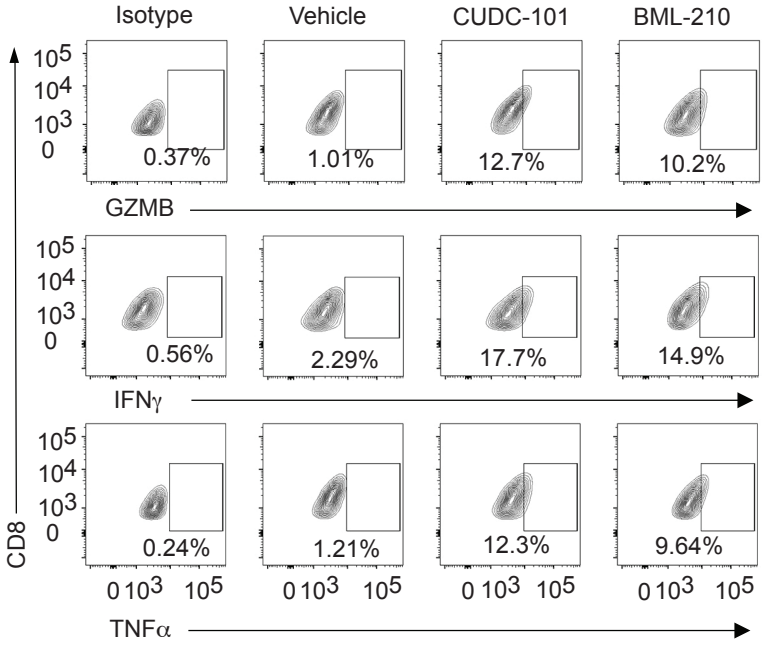
Isotype
Vehicle
CUDC-101
BML-210
GZMB
0.37%
1.01%
12.7%
10.2%
IFNγ
0.56%
2.29%
17.7%
14.9%
TNFα
0.24%
1.21%
12.3%
9.64%
CD8

c

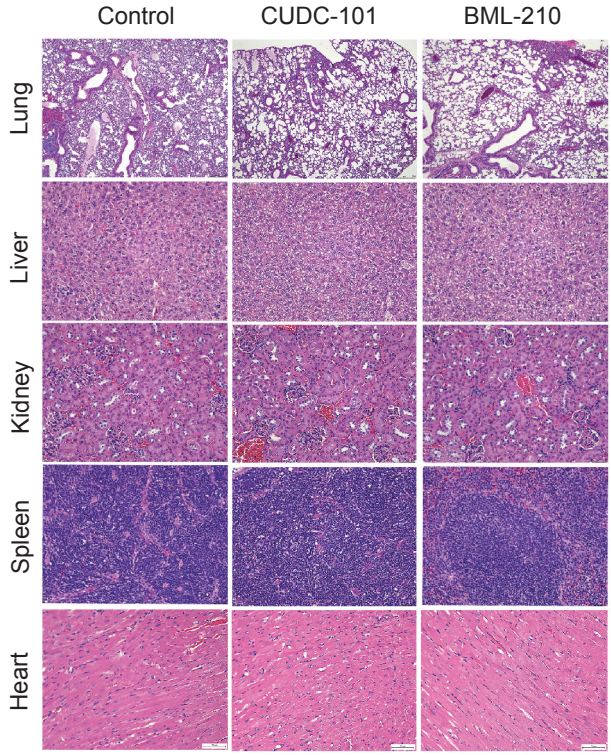
Control
CUDC-101
BML-210
Lung
Liver
Kidney
Spleen
Heart
Scale bar = 75 μm

d

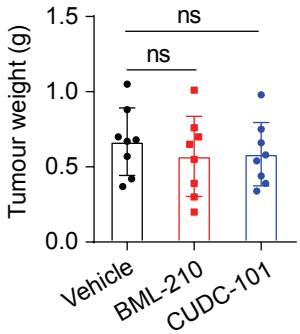
Tumour weight (g)
ns
ns
Vehicle
BML-210
CUDC-101

Supplementary Fig. 4 | Anti-tumour effects of BML-210 and CUDC-101 in mouse breast tumour models

a, Flow cytometry gating strategy for analysis of immune cells from EO771 tumours in C57BL/6 mice. **b,** Representative flow cytometry data showing active $CD8^+$ T cells in the EO771 tumours with vehicle control or drug treatment, indicated by positivity for GZMB, IFNγ and TNF-α. **c,** H&E staining images of heart, spleen, kidney, liver and lung from the mice treated with vehicle control, BML-210 or CUDC-101. Sample slides were examined in blind by a professional pathologist. The conclusion is that no visible differences were observed between control and drug treatment groups. One million of events per cell sample were collected for flow cytometry analysis. **d,** Weight of the EO771 tumours from the tumour-bearing immunodeficient nude mice treated with vehicle control, BML-210 (20 mg kg^{-1}), or CUDC-101 (20 mg kg^{-1}). Tumours from immunodeficient mice were harvested at day 18 post injection. One-way ANOVA test was used for statistical analysis. Data are presented as mean ± SD. ns, no significance.

a

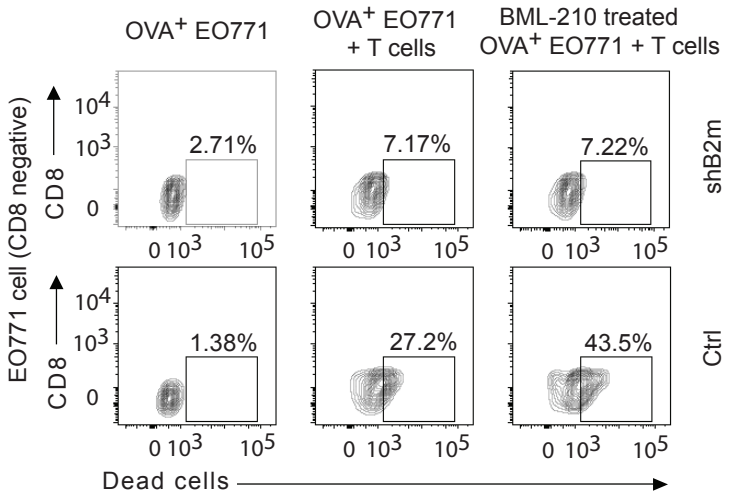
OVA+ EO771
OVA+ EO771 + T cells
BML-210 treated OVA+ EO771 + T cells
shB2m
Ctrl
EO771 cell (CD8 negative)
CD8
Dead cells
2.71%
7.17%
7.22%
1.38%
27.2%
43.5%

b

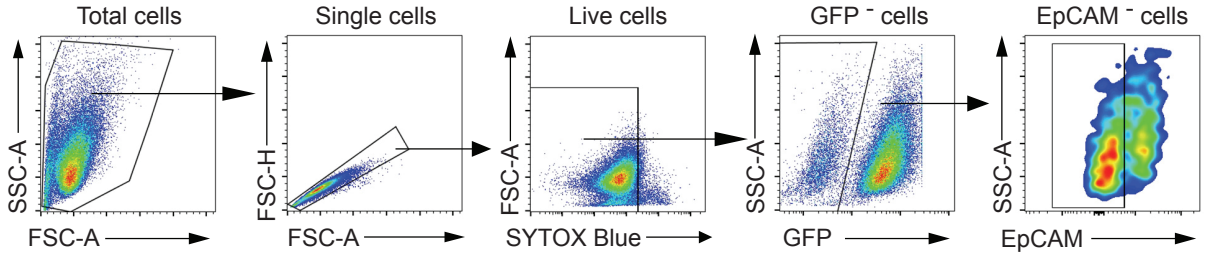
Total cells
Single cells
Live cells
GFP - cells
EpCAM - cells
SSC-A
FSC-A
FSC-H
SYTOX Blue
GFP
EpCAM

c

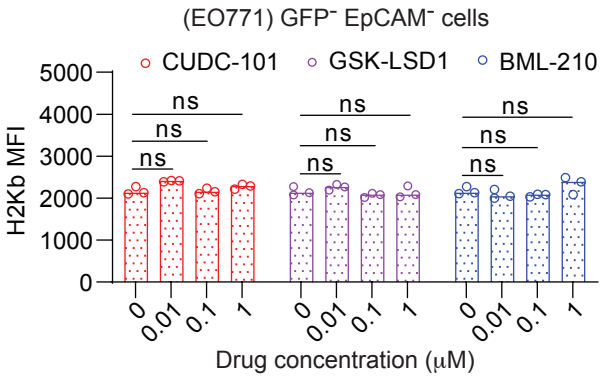
(EO771) GFP- EpCAM- cells
CUDC-101
GSK-LSD1
BML-210
H2Kb MFI
ns
Drug concentration (μM)

d

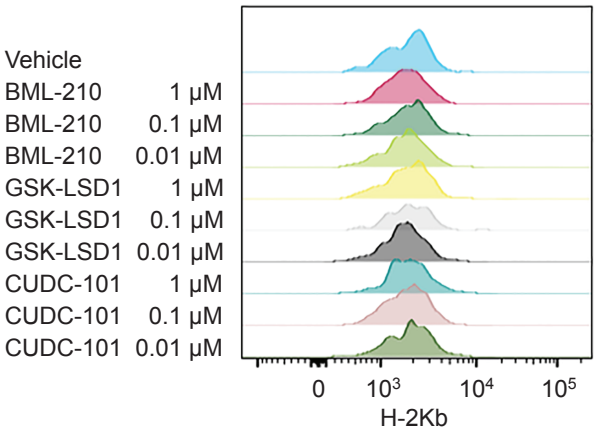
Vehicle
BML-210 1 μM
BML-210 0.1 μM
BML-210 0.01 μM
GSK-LSD1 1 μM
GSK-LSD1 0.1 μM
GSK-LSD1 0.01 μM
CUDC-101 1 μM
CUDC-101 0.1 μM
CUDC-101 0.01 μM
H-2Kb

Supplementary Fig. 5 | Drug candidates do not promote MHC-I associated antigen presentation of non-tumour cells from tumour organoids.

a, Representative flow cytometry data showing the death proportion of the OVA^+ EO771 tumour cells with and without B2M shRNA knockdown in the tumour organoids. Data from 3 biologically parallel experiments were analyzed using one-way ANOVA and presented as mean ± SD. **b,** Flow cytometry gating strategy for the analysis of GFP^-EPCAM^- cells from $GFP^+Luc^+OVA^+$ EO771 tumour organoids. **c,** Quantitative analysis of H-2Kb levels on the non-tumour cells (GFP^-EpCAM^-) cells from the $GFP^+Luc^+OVA^+$ EO771 tumour organoids treated with drug candidates. Data from 3 biologically parallel experiments were analyzed using Two-way ANOVA and presented as mean ± SD. ns, no significance. **d,** Representative flow cytometry data showing H-2Kb levels on the non-tumour cells (GFP^-EpCAM^-) cells from the $GFP^+Luc^+OVA^+$ EO771 tumour organoids treated with drug candidates.

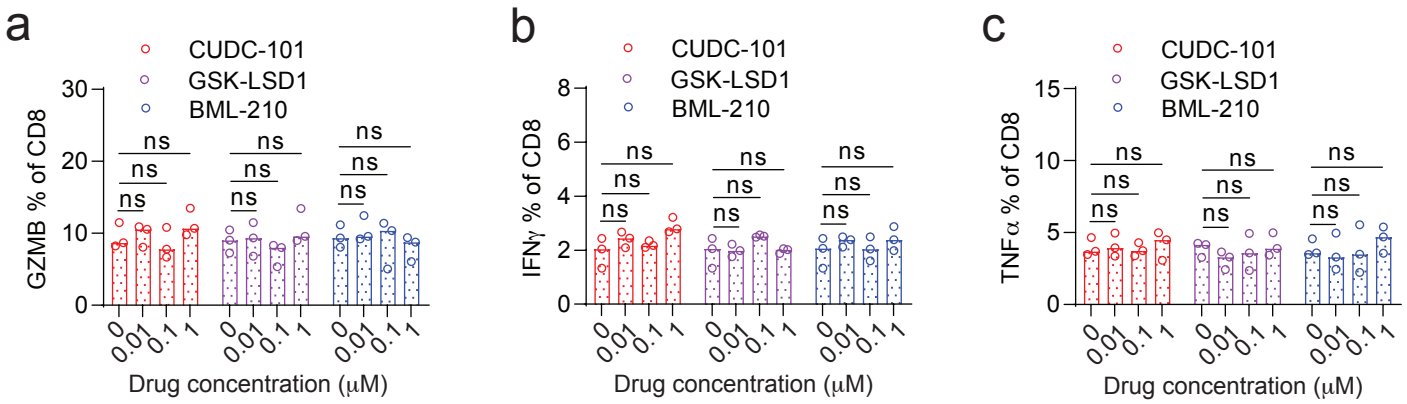
a
CUDC-101
GSK-LSD1
BML-210
GZMB % of CD8
Drug concentration (μM)
b
IFNγ % of CD8
c
TNFα % of CD8
ns

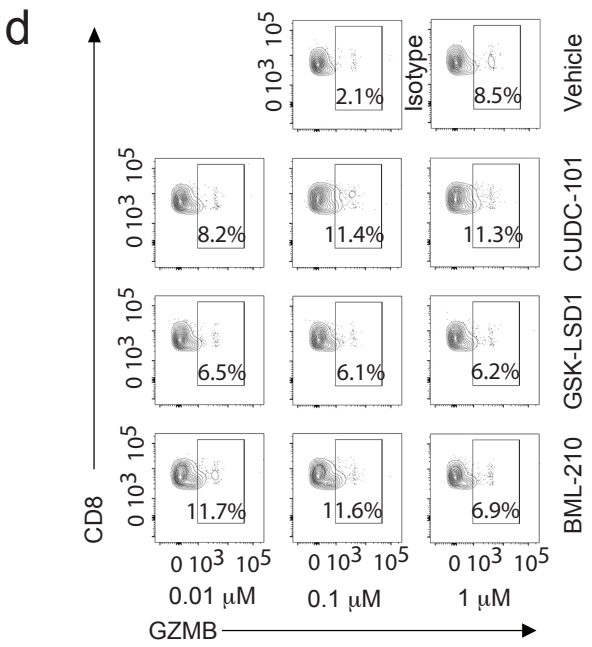
d
Isotype
Vehicle
CUDC-101
GSK-LSD1
BML-210
CD8
GZMB
0.01 μM
0.1 μM
1 μM
2.1%
8.5%
8.2%
11.4%
11.3%
6.5%
6.1%
6.2%
11.7%
11.6%
6.9%

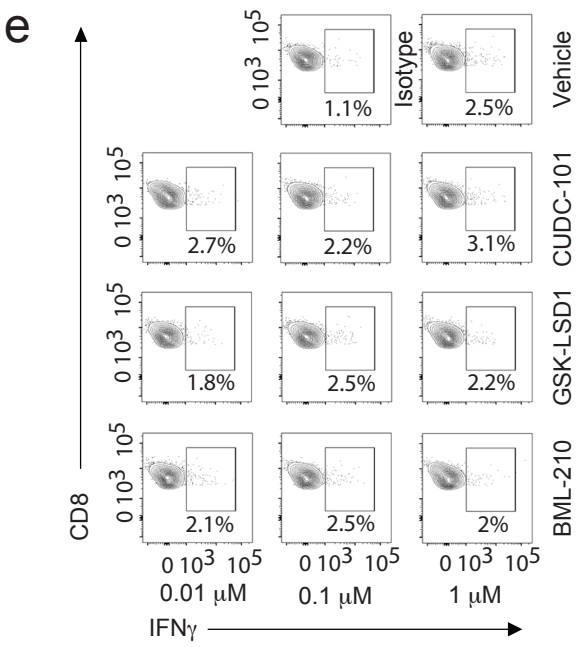
e
Isotype
Vehicle
CUDC-101
GSK-LSD1
BML-210
CD8
IFNγ
0.01 μM
0.1 μM
1 μM
1.1%
2.5%
2.7%
2.2%
3.1%
1.8%
2.5%
2.2%
2.1%
2.5%
2%

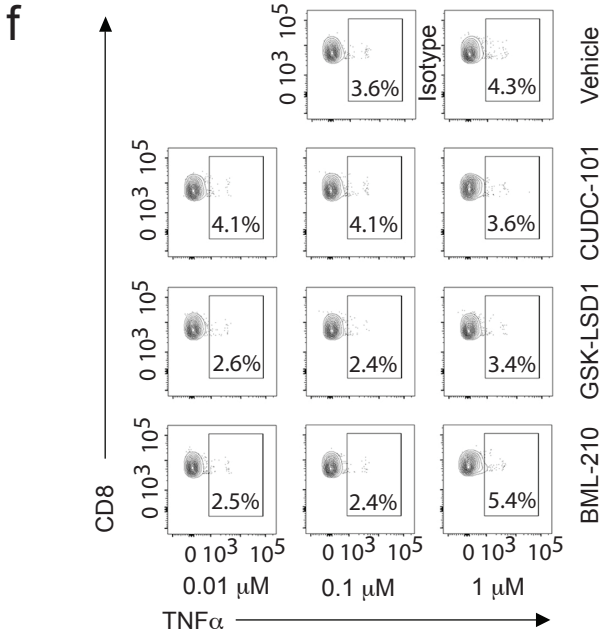
f
Isotype
Vehicle
CUDC-101
GSK-LSD1
BML-210
CD8
TNFα
0.01 μM
0.1 μM
1 μM
3.6%
4.3%
4.1%
4.1%
3.6%
2.6%
2.4%
3.4%
2.5%
2.4%
5.4%

Supplementary Fig. 6 | Drug candidates do not directly affect cytokine expression levels in $CD8^+$ T cells.

a-c, GZMB (**a**), IFNγ (**b**) and TNF-α (**c**) expression levels in the $CD8^+$ T cells treated with CUDC-101, GSK-LSD1 or BML-210 at indicated concentrations. $CD8^+$ T cells were isolated from the spleen of OT-I transgenic mouse. **d-f,** Representative flow cytometry data showing GZMB (**a**), IFNγ (**b**) and TNF-α (**c**) expression levels in the $CD8^+$ T cells. Data (**a**-**c**) from three biologically parallel experiments were analyzed using Two-way ANOVA and presented as mean ± SD. ns, no significance.

a

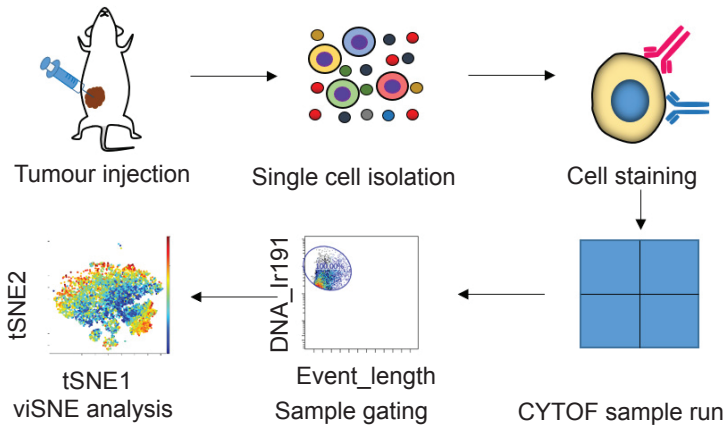

Mass cytometry analysis of immune cells in the tumour

b

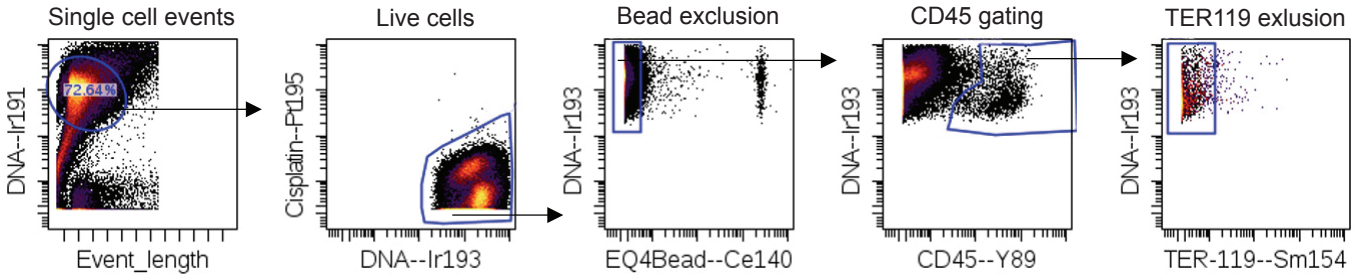

c

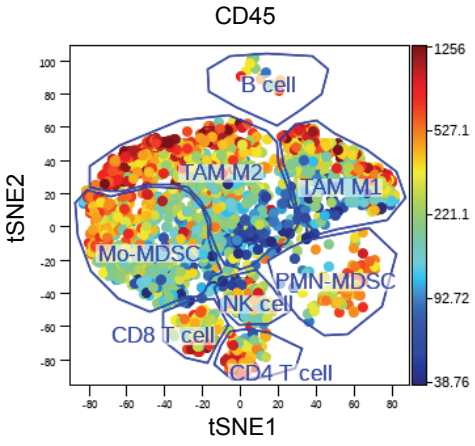

d

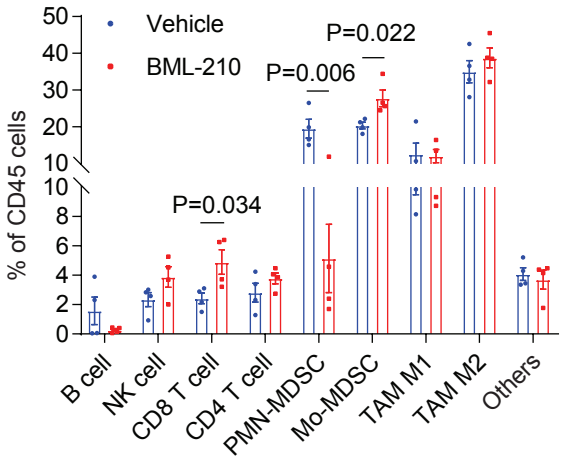

Supplementary Fig. 7 | Mass cytometry (CyTOF) analysis of immune cell profiles in EO771 tumours upon BML-210 treatment.

a, CyTOF gating strategy for immune cells in EO771 tumours harvested from the tumour-bearing C57BL/6 mice with and without BML-210 drug treatment. A panel of 26 antibodies were used for CyTOF analysis (**Supplementary Table 2**). The data were analyzed using viSNE in the Cytobank platform. **b,** Gating Strategy for immune cells in EO771 tumours before the viSNE analysis. **c,** The different immune cell subtypes displayed in tSNE plot. **d,** The proportion of different immune cell subtypes in the control and BML-210-treated breast tumours, determined by viSNE analysis. Data were analyzed using Two-way ANOVA and presented as mean ±.

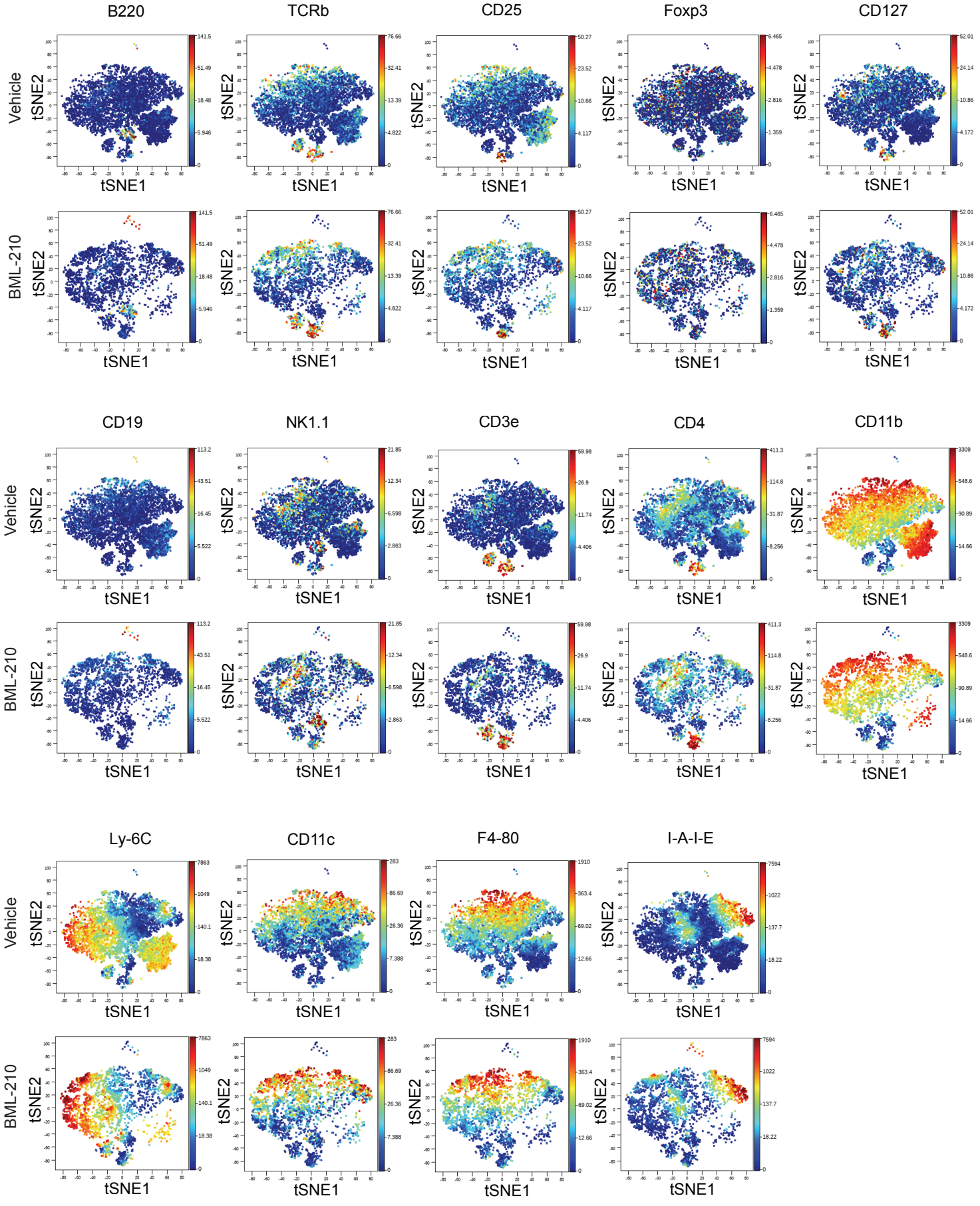
B220
TCRb
CD25
Foxp3
CD127
CD19
NK1.1
CD3e
CD4
CD11b
Ly-6C
CD11c
F4-80
I-A-I-E
Vehicle
BML-210
tSNE1
tSNE2

Supplementary Fig. 8 | Mass cytometry (CyTOF) single channel plots of immune cell profiles in EO771 tumours upon BML-210 treatment.

tSNE representation of immune cell subtypes in the EO771 tumours with control or BML-210 treatment, analyzed by viSNE analysis via the Cytobank platform.

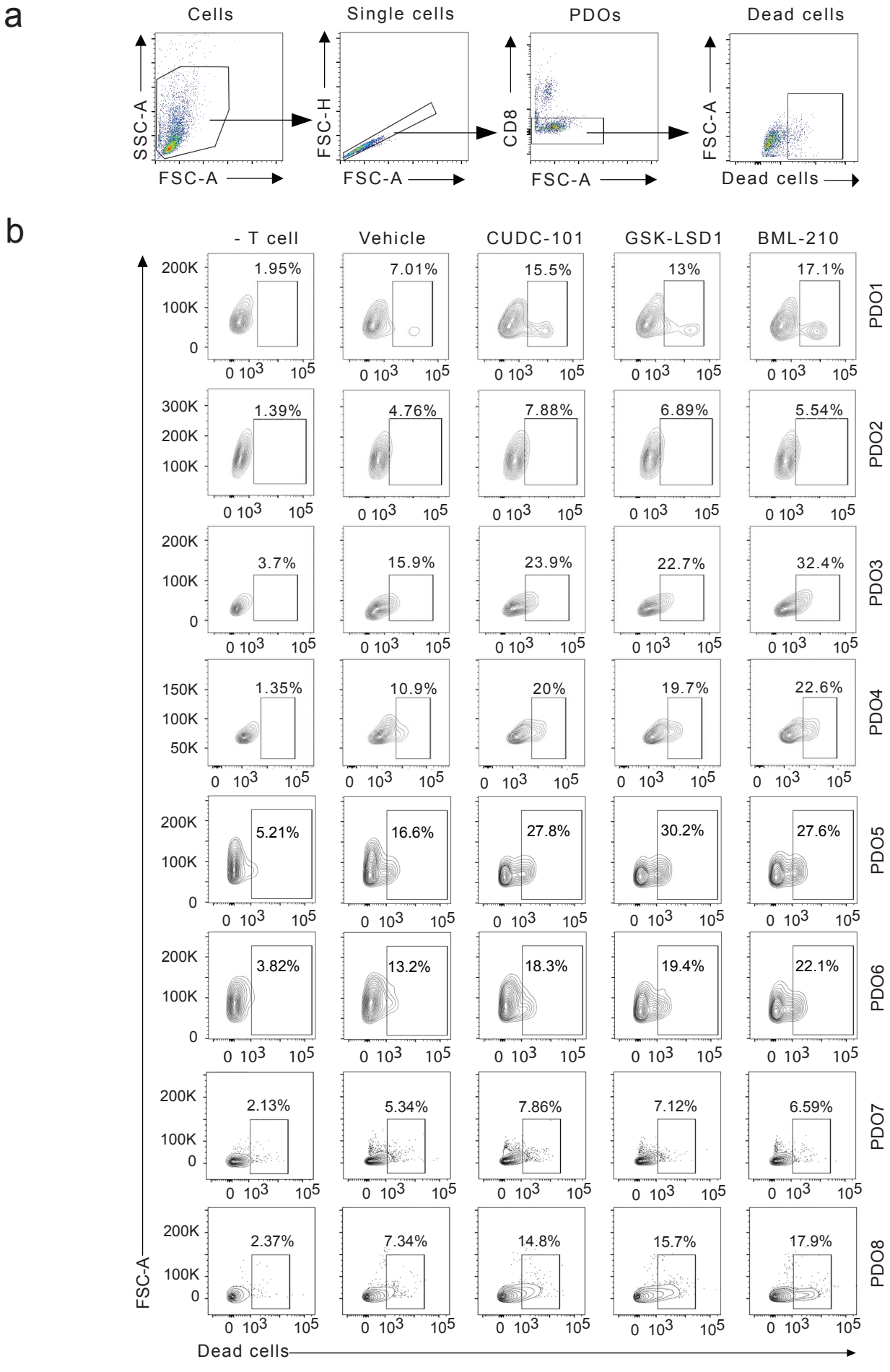
a
Cells
Single cells
PDOs
Dead cells
SSC-A
FSC-A
FSC-H
FSC-A
CD8
FSC-A
FSC-A
Dead cells
b
- T cell
Vehicle
CUDC-101
GSK-LSD1
BML-210
PDO1
PDO2
PDO3
PDO4
PDO5
PDO6
PDO7
PDO8
1.95%
7.01%
15.5%
13%
17.1%
1.39%
4.76%
7.88%
6.89%
5.54%
3.7%
15.9%
23.9%
22.7%
32.4%
1.35%
10.9%
20%
19.7%
22.6%
5.21%
16.6%
27.8%
30.2%
27.6%
3.82%
13.2%
18.3%
19.4%
22.1%
2.13%
5.34%
7.86%
7.12%
6.59%
2.37%
7.34%
14.8%
15.7%
17.9%
FSC-A
Dead cells

Supplementary Fig. 9 | The effect of drug treatment on the cytotoxicity of autologous $CD8^+$ T cell on patient-derived breast tumour organoids.

a, Flow cytometry gating strategy for dead tumour cells in PDOs killed by $CD8^+$ T cells. **b,** Representative flow cytometry data showing the death proportion of tumour cells in CUDC-101, GSK-LSD1 and BML-210 treated PDOs. PDO1-8 refers to 8 PDOs generated from fresh breast tumour tissue samples from 8 patients.

Supplementary Table 1. Epigenetic inhibitors library (Cayman Chemical)

Item No.11076; Batch No. 0522205

NUMBER	DRUG NAME	CATALOG
1	(+)-Abscisic Acid	10073
2	3-amino Benzamide	10397
3	SB939	10443
4	PCI 34051	10444
5	4-iodo-SAHA	10495
6	Sirtinol	10523
7	C646	10549
8	Tubastatin A (trifluoroacetate salt)	10559
9	Garcinol	10566
10	Ellagic Acid	10569
11	Scriptaid	10572
12	Apicidin	10575
13	HC Toxin	10576
14	UNC0321 (trifluoroacetate salt)	10582
15	(−)-Neplanocin A	10584
16	Cl-Amidine (trifluoroacetate salt)	10599
17	F-Amidine (trifluoroacetate salt)	10610
18	JGB1741	10641
19	coumarin-SAHA	10671
20	I-BET762	10676
21	UNC0638	10734
22	Phthalazinone pyrazole	10735
23	Isoliquiritigenin	10739
24	CCG-100602	10787
25	CAY10669	10974
26	Zebularine	10975
27	Delphinidin (chloride)	11012
28	ITF 2357	11045
29	UNC0631	11084
30	UNC0646	11085
31	Methylstat (hydrate)	11091
32	3-Deazaneplanocin A (hydrochloride)	11102
33	Suramin (sodium salt)	11126
34	Nicotinamide	11127
35	2,4-Pyridinedicarboxylic Acid	11138
36	PFI-1	11155
37	5-Azacytidine	11164
38	SGI-1027	11165
39	Decitabine	11166

40	I-BET151	11181
41	(+)-JQ1	11187
42	(−)-JQ1	11232
43	BSI-201	11304
44	1-Naphthoic Acid	11322
45	Sodium 4-Phenylbutyrate	11323
46	Rucaparib (phosphate)	11570
47	IOX1	11572
48	MI-2 (hydrochloride)	11620
49	MI-nc (hydrochloride)	11621
50	Gemcitabine	11690
51	Lomeguatrib	11732
52	GSK4112	11931
53	Octyl-α-ketoglutarate	11970
54	Daminozide	12033
55	GSK-J1 (sodium salt)	12054
56	GSK-J2 (sodium salt)	12056
57	GSK-J4 (hydrochloride)	12073
58	CI-994	12084
59	CPTH2 (hydrochloride)	12086
60	Etoposide	12092
61	Lestaurtinib	12094
62	Butyrolactone 3	12095
63	Valproic Acid (sodium salt)	13033
64	Tenovin-1	13085
65	Tenovin-6	13086
66	Sodium Butyrate	13121
67	BIX01294 (hydrochloride hydrate)	13124
68	Anacardic Acid	13144
69	AGK2	13145
70	CAY10603	13146
71	Splitomicin	13168
72	CBHA	13172
73	M 344	13174
74	Oxamflatin	13176
75	Salermide	13178
76	Mirin	13208
77	Pimelic Diphenylamide 106	13212
78	KD 5170	13214
79	Panobinostat	13280
80	MS-275	13284
81	HNHA	13295
82	RG-108	13302
83	2’,3’,5’-triacetyl-5-Azacytidine	13373

84	S-Adenosylhomocysteine	13603
85	UNC0224	13631
86	Chidamide	13686
87	Tubacin	13691
88	3-Deazaneplanocin A	13828
89	Sinefungin	13829
90	Pyroxamide	13870
91	N-Oxalylglycine	13944
92	WDR5-0103	13945
93	EPZ005687	13966
94	SGC0946	13967
95	UNC1215	13968
96	AK-7	14004
97	GSK343	14094
98	Bromosporine	14119
99	GSK2801	14120
100	SIRT1/2 Inhibitor IV	14407
101	I-CBP112 (hydrochloride)	14468
102	SGC-CBP30	14469
103	UNC0642	14604
104	UNC1999	14621
105	I-PFI-2 (hydrochloride)	14678
106	HPOB	15066
107	2-hexyl-4-Pentynoic Acid	15205
108	PFI-3	15267
109	JIB-04	15338
110	CAY10683	15403
111	GSK126	15415
112	CPI-203	15479
113	6-Thioguanine	15774
114	Tubastatin A	15785
115	3,3’-Diindolylmethane	15927
116	OTX015	15947
117	5-Methylcytidine	16111
118	AGK7	16152
119	5-Methyl-2’-deoxycytidine	16166
120	EPZ5676	16175
121	MC 1568	16265
122	α-Hydroxyglutaric Acid (sodium salt)	16374
123	S-(5’-Adenosyl)-L-methionine (tosylate)	16376
124	RVX-208	16424
125	CUDC-101	16426
126	LAQ824	16427
127	Nullscript	16433

128	GSK-LSD1 (hydrochloride)	16439
129	RGFP966	16917
130	BRD73954	16919
131	*trans*-Resveratrol	70675
132	DMOG	71210
133	Trichostatin A	89730
134	CAY10398	89740
135	RSC-133	9001839
136	BML-210	10005019
137	Piceatannol	10009366
138	CAY10591	10009797
139	EX-527	10009798
140	SAHA	10009929
141	2-PCPA (hydrochloride)	10010494

Supplementary Table 2. Antibody panel for CyTOF analysis

	Marker	Clone	Tag	Cat. #	Sample (µl)
1	CD45	30- F11	89Y	3089005B	0.25
2	I-A/I-E	M5/114.15.2	209Bi	3209006B	0.5
3	CD274/PD-L1	10F.9G2	153Eu	3153016B	0.25
4	CD3e	145-2C11	152Sm	3152004B	0.25
5	CD8a	53-6.7	146Nd	3146003B	0.5
6	CD25	3C7	150Nd	3150002B	0.25
7	CD127/IL7Ra	A7R34	175Lu	3175006B	0.5
8	CD62L	MEL-14	160Gd	3160008B	0.17
9	CD69	H1.2F3	145Nd	3145005B	0.5
10	TCRb	H57-597	143Nd	3143010B	0.5
11	CD44	IM7	171Yb	3171003B	0.2
12	CD11b	M1/70	148Nd	3148003B	0.17
13	CD11c	N418	142^{Nd}	3142003B	0.5
14	F4/80	BM8	159Tb	3159009B	0.25
15	Ly-6C	HK1.4	162Dy	3162014B	0.2
16	Ly-6G	1A8	141Pr	3141008B	0.5
17	NK1.1	PK136	170Er	3170002B	0.5
18	CD45R/ B220	RA3-6B2	176Yb	3176002B	0.5
19	CD19	6D5	149Sm	3149002B	0.5
20	TER-119	TER-119	154Sm	3154005B	0.25
21	EpCAM	G8.8	166Er	3166014B	0.25
22	Vimentin	RV202	156Gd	315602A	0.25
23	CCR7	4B12	164Dy	3164013A	0.25
24	LAG3	C9B7W	174Yb	3174019B	0.25
25	CD4	RM4-5	172Yb	3172003B	0.5
26	CD206	C068C2	169Tm	3169021B	0.25

Supplementary Table 3. Clinical information of human breast cancer samples.

Patient samples	Sex	Age	Surgery	Diagnosis
1	F	61	mastectomy	Papillary carcinoma
2	F	34	mastectomy	Inflammatory breast cancer
3	F	34	mastectomy	Triple negative breast cancer
4	F	62	mastectomy	Invasive ductal carcinoma (ER+)
5	F	68	mastectomy	Invasive ductal carcinoma (ER/PR +, HER2-)
6	F	85	mastectomy	Invasive ductal carcinoma (ER/PR+, HER2 equivocal)
7	F	48	mastectomy	Invasive ductal carcinoma (TNBC)
8	F	55	mastectomy	Invasive ductal carcinoma (ER+, PR-, HER2-)
9	F	65	mastectomy	Invasive ductal carcinoma (ER+, PR+, HER2-)
10	F	59	Partial mastectomy	Recurrent invasive ductal carcinoma (ER+/PR+)

Supplementary Table 4. Mouse breast tumour organoid culture medium

Products	Name	Company	Catalog #	Concentration
1	GlutaMAX Supplement	Thermo Fisher	35050061	1x
2	B-27™ Supplement (50X), serum free	Sigma	17504044	1x
3	N-acetyl-L-cysteine	Sigma	A7250-5G	1 mM
4	Recombinant murine EGF	PeproTech	315-09	5 μg/ml
5	R spondin-1	Sigma	SRP6487-10UG	0.5 μg/ml
6	Noggin	PeproTech	120-10C	0.1 μg/ml
7	FGF10	Biolegend	751004	10 ng/ml
8	Recombinant murine FGF	Sigma	PMG0034	5 ng/ml
9	A 83-01	Tocris	2939	500 nM
10	SB 202190	Sigma	S7067	10 μM
11	Penicillin/Streptomycin	Corning	30-002-CI	1:100
12	Fetal bovine serum	Sigma	12103C-500ML	10%
13	DMEM/F12	Corning	10092CM	500 ml

Supplementary Table 5. RT-qPCR Primers

Mouse primers		Human primers	
Primer Name	**Sequence 5' to 3'**	**Primer Name**	**Sequence 5' to 3'**
B2m qF	TTCTGGTGCTTGTCTCACTGA	B2M qF	GAGGCTATCCAGCGTACTCCA
B2m qR	CAGTATGTTCGGCTTCCCATTC	B2M qR	CGGCAGGCATACTCATCTTTT
Calr qF	TGGCTGCTCCCAATAATGTCT	CALR qF	CCTGCCGTCTACTTCAAGGAG
Calr qR	GAGGGTAGTGACCAAAAGATGG	CALR qR	GAACTTGCCGGAACTGAGAAC
Itgav qF	CCGTGGACTTCTTCGAGCC	ITGAV qF	ATCTGTGAGGTCGAAACAGGA
Itgav qR	CTGTTGAATCAAACTCAATGGGC	ITGAV qR	TGGAGCATACTCAACAGTCTTTG
Sec22b qF	CTGACGATGATCGCCCGTG	CTSV qF	CGTGACGCCAGTGAAGAATCA
Sec22b qR	TGCTTAGCCTGACTCTGATACTG	CTSV qR	CGCTCAGTGAGACAAGTTTCC
Sec23a qF	AGATGGGGTCCGGTTCAGTT	SEC22B qF	CCGGGACCTTCAACAATATCAG
Sec23aqR	GGTAGGTCGGGTCTCTCCTT	SEC22B qR	GCAAAAGCCAACTTCTTAGGGA
Sec24a qF	TCCTGTCCACAATACACTGATGT	SEC23A qF	GGAGTCCGATTTAGTTGGAATGT
Sec24a qR	GAACCACCGTAGTTCGACTGT	SEC23A qR	AGGTCTCTCTTTCAGTGGTGT
Sec24c qF	CTGGCCGGAATGCAGATCAG	SEC24A qF	ATGTCCCAGCCGGGAATAC
Sec24c qR	TGAGGATAGGAGCCGTATGGA	SEC24A qR	AGGACCGTTGGTGTAGGGAG
Sec24d qF	GGAGAGGTCTTTGTTCCTTTGTT	SEC24C qF	AACGTCAACCAGTCAGTTCCA
Sec24d qR	GTCTCTGTTCTTGAGCTTCCC	SEC24C qR	GGCTCCATAGGGAATGGCG
Psmb4 qF	ATGGAAGCGTTTTGGGAGTCA	SEC24D qF	GTCAACAAGGTTACGTGGCTA
Psmb4 qR	GTTCTGGGTCCGAGTGATGG	SEC24D qR	TAGTGCCCATAATGAGGTGGA
Psmd2 qF	TGGACGAGACAAGACACCC	PSMD8 qF	GCCGTAAATCAGGCGGTCT
Psmd2 qR	CTCCACGAGCATCTCCAGTTC	PSMD8 qR	GCCCTTGAGTTGCTCGTACA
Psmd8 qF	GGCATGTACGAGCAACTCAAG	PSMD11 qF	GCCTCCATCGACATCCTCC
Psmd8 qR	GCTCAAGCAGAACCAACTTCA	PSMD11 qR	GAGCTGCTTTAGCCTTGCTG
Psme4 qF	AGCGTCAACAAGATAAGAATGCT	PSMB4 qF	GAAGCGTTTTTGGGGTCGC
Psme4 qR	GCCCGATTCCTATATGCTCAAA	PSMB4 qR	GAGTGGACGGAATGCGGTA
Psmd11 qF	GCAGGAGGTCGAGCTATGTTT	HLA-A qF	AAAAGGAGGGAGTTACACTCAGG
Psmd11 qR	TGAGAACCCAAATGCAATGCTT	HLA-A qR	GCTGTGAGGGACACATCAGAG
H-2k1 qF	ACCAGCAGTACGCCTACGA		
H-2k1 qR	AACCAGAACAGCAACGGTCG		

Supplementary Table 6. Reagents and resources

REAGENT or RESOURCE	SOURCE	CATALOG
Antibodies		
iFluor488-conjugated Phalloidin	Abcam	ab176753
Rbmab-EPCAM antibody	Abcam	ab32392
anti-mouse PD-1	Bioxcell	BE0146; Clone: RMP1-14
Rat IgG2a isotype control	Bioxcell	BE0089
Anti-CD4	Bioxcell	BE0003-1; Clone: GK1.5
Anti-CD8	Bioxcell	BE0004-1; Clone: 53-6.72
beta-2 microglobulin antibody	Abcam	Ab175031
Beta-Actin antibody	Abgent	AM1829b
anti-mouse CD8α (D4W2Z) antibody, rabbit monoclonal	Cell Signaling Technology	98941S
Cleaved caspase 3 (Asp175) antibody	Cell signaling Technology	9661S
mouse Ki-67 antibody	Cell signaling Technology	12202S
AF594-conjugated anti-mouse CD31	Biolegend	102520
APC-conjugated anti-mouse CD140a	Biolegend	135907
PE-conjugated anti-mouse CD326	Biolegend	118206
AF647-conjugated anti-mouse CD326	Biolegend	118212
FITC-conjugated Mouse α-Smooth Muscle Actin	GeneTex	GTX72531
AF647-conjugated Donkey anti-rabbit IgG	Biolegend	406414
APC/Cy7-conjugated anti-human CD8a	Biolegend	300926
APC-conjugated anti-human IFNγ	Biolegend	502512
PE-conjugated anti-human TNFα	Biolegend	502909
APC-conjugated anti-mouse IFNγ	Biolegend	505810
PE-conjugated anti-mouse TNFα	Biolegend	506306
PerCP/Cyanine5.5-conjugated anti-human/mouse Granzyme B	Biolegend	372212
BV605-conjugated anti-mouse CD45	Biolegend	103139
PE/Cy7-conjugated anti-mouse CD3	Biolegend	100220
AF700-conjugated anti-mouse CD4	Biolegend	100430
APC/Cy7-conjugated anti-mouse CD8	Biolegend	100714
APC-conjugated anti-mouse CD8	Biolegend	126613
PE-conjugated anti-mouse CD11b	Biolegend	101208
AF647-conjugated anti-mouse CD11c	Biolegend	117312
PerCP/Cy5.5-conjugated anti-mouse Fn/80	Biolegend	123128
BV421-conjugated anti-mouse I-A/I-E	Biolegend	107631
BV650-conjugated anti-mouse CD19	Biolegend	115541
PE-conjugated anti-mouse H-2Kb bound to SIINFEKL antibody	Biolegend	141603

APC-conjugated anti-mouse H-2Kb bound to SIINFEKL antibody	Biolegend	141606
FITC-Anti-Human HLA-A,B,C antibody	Biolegend	311403
FITC-Anti-Human HLA-A2 antibody	Biolegend	343303
FITC-conjugated anti-H-2Kb	Biolegend	116505
FITC-conjugated anti-Rat IgG	Biolegend	407505
FITC-conjugated anti-mouse IgG	Biolegend	406001
SYTOX™ Blue dead cells	Invitrogen	2078615
Chemicals, Peptides, Proteins and Consumables		
Matrigel	Corning	356255
Mouse IL2	Biolegend	575402
Human IL2	Biolegend	589102
Image-iT™ Green Hypoxia reagent	Invitrogen	I14833
phorbol 12-myristate 13-acetate	Sigma-Aldrich	16561-29-8
Ionomycin	Sigma-Aldrich	56092-82-1
Brefeldin A	Biolegend	420601
Cell strainers (40 µm)	Fisher Scientific	07201430
Cell strainers (70 µm)	Fisher Scientific	07201431
Cell strainers (100 µm)	Fisher Scientific	07201432
Cell strainers (150 µm)	pluriStrainer	43-50150-03
Cell strainers (300 µm)	pluriStrainer	43-50300-03
Cell strainers (500 µm)	pluriStrainer	43-50500-03
Mouse tumour dissociation kit	Milenyi Biotec	130-096-730
Human tumour dissociation kit	Milenyi Biotec	130-095-929
Human CD8+ magnetic beads	Milenyi Biotec	130-045-201
Mouse CD8+ magnetic beads	Milenyi Biotec	130-117-044
Dynabeads Human T activator CD3/CD28	Gibco	11131D
Dynabeads Mouse T activator CD3/CD28	Gibco	11452D
BD comp Beads Negative Control	BD Biosciences	51-90-9001291
BD comp Beads Anti-Mouse Ig,κ	BD Biosciences	51-90-9001229
BD comp Beads Anti-Rat and Anti-Hamster Ig,κ	BD Biosciences	51-90-9000949
low-attachment surface 96-well microplate	Corning	3474
low-attachment surface 24-well microplate	Corning	3473
low-attachment surface 6-well microplate	Corning	3471
8-Well glass EZ Slide	Millicell	R8AA09916
RNeasy mini-isolation kit	QIAGEN	157029493
QIAseq FastSelect rRNA Removal HMR Kit	QIAGEN	334387
KAPA RNA Hyper Prep Kit	Roche Corporate	KK8541
QscriptXLT cDNA super Mix	Quantabio	66141329
SYBR Green fastmix low Rox	TaKaRa	4385610
Lipofectamine 3000 reagent	Thermo Fisher Scientific	25530049
Premix WST-1 assay	TaKaRa	MK400
Prolong Gold anti-fade medium	Invitrogen	P36930
Cytofix/cytoperm fixation/permeabilization kit	BD Biosciences	554714
TRIzol	Ambion	260808

RBC lysis buffer(10X)	Biolegend	420301
Dual-luciferase report 1000 assay system	Promega	E1980
ELISA MAX™ Deluxe Set Human TNF-α	Biolegend	430204
ELISA MAX™ Deluxe Set Mouse TNF-α	Biolegend	430904
ELISA MAX™ Deluxe Set Human IFN-γ	Biolegend	430104
ELISA MAX™ Deluxe Set Mouse IFN-γ	Biolegend	430804
Epigenetic drug library	Cayman Chemical	11071
Cells and Cell Lines		
MDA-MB-468	ATCC	Cat# HTB-132; RRID:CVCL_0419
HEK293T	ATCC	Cat# CRL-3216; RRID: CVCL_0063
EO771	CH3 BioSystems	Cat# 940001; RRID: CVCL_GR23
Anti-NY-ESO-1 human CD8+ T cells	ASTARTE Biologics	1093-4245MA19
Mouse beta-2-microglobulin (B2M) shRNA bacterial Glycerol stock	Sigma-Aldrich	SHCLNG-NM_00935, TRCN0000288438
Software and Algorithms		
FlowJo	N/A	FlowJo version 10.6.0
GraphPad	N/A	GraphPad Prism 8.0 software
Matlab	MathWorks Inc.	Version 8.2.1, R2016b
IMARIS	N/A	IMARIS x64 8.1.2
ImageJ	N/A	ImageJ (64bit 1.50e)
Mass Cytometry	Cytobank	https://cytobank.org/
R	N/A	https://www.R-project.org/
Gene Set Enrichment Analysis (GSEA)	N/A	http://software.broadinstitute.org/gsea/